



13th International Conference on Greenhouse Gas Control Technologies, GHGT-13, 14-18  
November 2016, Lausanne, Switzerland

## Analytical approach for modeling of multi well CO<sub>2</sub> injection

Morgan Robinson<sup>a</sup> and Yuri Leonenko<sup>b,c,\*</sup>

<sup>a</sup>Department of Biology, <sup>b</sup>Department of Earth and Environmental Sciences, <sup>c</sup>Department of Geography and Environmental Management,  
University of Waterloo, Waterloo, Ontario, N2L 3G1, Canada

---

### Abstract

Disposal of carbon dioxide (CO<sub>2</sub>) into underground geological formations is considered a viable strategy for the mitigation of global warming. It aims to reduce greenhouse gases emitted from point sources such as power plants. In order to select and evaluate a potential storage formation, many reservoir properties such as porosity, permeability, lateral and vertical extents, and a variety of residual fluid properties are considered. Injection design, which includes the placement of injectors and their flow rates, should be chosen to optimize injection capacity. One of the most important considerations to be addressed during design stage of sequestration is evaluation of pressure behaviour inside the reservoir during and after injection as the sequestered CO<sub>2</sub> increases the pressure within the formation. In order to maintain the integrity of the reservoir the pressure needs to be maintained below the fracture pressure, typically at least 10% below. Thus evaluation of reservoir pressure is essential to ensure the reservoir remains under the maximum allowable pressure while sequestering the maximum amount of CO<sub>2</sub> for long term storage in the reservoir. The optimal injection rates within a multi well injection site occur when the bottom-hole pressure at each injection site is at the maximum allowable pressure. In this study we present an analytical approach for modeling the pressure evolution during multi well CO<sub>2</sub> injection into saline aquifers and using the model modify the injection rates to optimize injection capacity within a formation. We show that this optimization procedure significantly increases the capacity of formation as opposed to using the same injection rate at each wellbore.

© 2017 The Authors. Published by Elsevier Ltd. This is an open access article under the CC BY-NC-ND license (<http://creativecommons.org/licenses/by-nc-nd/4.0/>).

Peer-review under responsibility of the organizing committee of GHGT-13.

*Keywords:* multi well injection; aquifer; CO<sub>2</sub> sequestration

---

---

\* Corresponding author. Tel.: +1 (519) 888-4567 (Ex. 32160); fax: +1 (519) 746-8115.  
E-mail address: [leonenko@uwaterloo.ca](mailto:leonenko@uwaterloo.ca)

## 1. Introduction

In IPCC report [1] it was suggested that underground saline aquifers have a storage capacity of around  $2 \times 10^3$  gigaton (Gt) of carbon dioxide which is about two orders of magnitude higher than the total annual worldwide emissions, making it a potential disposal option. Although these formations offer high storage capacity, we showed previously [2, 3] that practical implementation to fill this capacity with CO<sub>2</sub> could be very challenging. In order to make disposal in underground aquifers a viable option to mitigate climate change, we should be able to sequester large quantities of CO<sub>2</sub> with scales of 10-30 Mt/year per injection site. Currently, the typical injection rates used in research studies and in field projects are around one megaton (Mt) per year. Larger, by order of magnitude, volumes of CO<sub>2</sub> injected within a short period of time (50-100 years) increase the reservoir pressure extremely fast which may lead to loss in integrity of the reservoir. Therefore, projected capacity of reservoir should be evaluated not by available pore space but by injection capacity, defined by how much carbon dioxide can be injected within a given period of time and within particular injection area.

Previously [2,3], we reported that increasing the number of injection wells in a formation does increase CO<sub>2</sub> injection capacity within a reservoir however if well placement and injection rates are not optimized the increase in injection capacity per well decreases exponentially with increasing well number due to well interference. We showed that changes in well placement configurations such as the spacing between wells, symmetric and asymmetric configurations as well as the removal of central wells has a pronounced effect on CO<sub>2</sub> injection capacity, for example the removal of a central well in a multi well injection site can increase injection capacity [4]. In this work we expand on these models and show that increasing the efficiency of CO<sub>2</sub> injection wells can be achieved by optimization of the injection rates within the well configuration. We provide analysis of two different test cases, one is from data provided in study [5], which was set at the Lawrence Berkeley National Laboratory, and the other is from data gathered from the Nisku aquifer in Alberta, Canada and provided by CMC (Carbon Management Canada).

### Nomenclature

$P$	Reservoir Pressure
$P_i$	Initial reservoir pressure
$r$	Radius
$r_w$	Well radius
$r_D$	Dimensionless radius; $r_D = r / r_w$
$q$	Injection rate
$E_i$	Exponential integral function
$k$	Formation permeability
$k_{rg}$	Gas relative permeability and gas relative permeability in dr region, ( $\overline{k_{rg}}$ at $S_g=1$ )
$k_{rw}$	Brine relative permeability and brine relative permeability in BL region, ( $\overline{k_{rw}}=1$ )
$h$	Reservoir thickness
$\phi$	Porosity
$S_w$	Brine saturation
$S_g$	Gas saturation
$S_{gr}$	Residual gas saturation
$S_{wr}$	Residual brine saturation
$\mu_w$	Brine viscosity
$\mu_g$	Gas viscosity

$\bar{\lambda}_g$	Gas endpoint mobility; $\bar{k}_{rg} / \mu_g$
$\lambda_g$	Gas mobility; $k_{rg} / \mu_g$
$\bar{\lambda}_w$	Brine endpoint mobility; $1 / \mu_w$
$\lambda_w$	Brine mobility; $k_{rw} / \mu_w$
$B_g$	CO <sub>2</sub> gas volume formation factor
$f_g$	Fractional flow
$c_r$	Reservoir compressibility
$c_g$	Gas compressibility
$c_w$	Brine compressibility
$c_t$	Total compressibility; $c_t = S_g c_g + (1 - S_g) c_w + c_r$
$c_{rg}$	Total compressibility of the gas region; $c_{rg} = c_g + c_r$
$\xi$	Dimensionless similarity form; $\xi = r_D^2 / 4t_D$
$\eta_{D2}$	Compressibility ratio at average S <sub>g</sub> ; $\eta_{D2} = c_{rg} / c_t$
$\eta_{D3}$	Diffusivity ratio at average S <sub>g</sub> ; $\eta_{D3} = c_{rg} \bar{\lambda}_w / c_t \lambda_g$
$F_{\lambda_g}$	Dimensionless total mobility; $F_{\lambda_g} = (\lambda_g + \lambda_w) / \bar{\lambda}_g$
$P_D$	Dimensionless Pressure; $P_D = 2\pi h k_{rg} (P - P_i) / q \mu_g B_g$
$\mathcal{E}$	Dimensionless injection rate; $\mathcal{E} = q \mu_g B_g c_{rg} / 4\pi h k_{rg}$
$t_D$	Dimensionless time; $P_D = k \bar{k}_{rg} t / \mu_g r_w^2 \phi c_{rg}$

## 2. Modeling

### 2.1 Approach

There is a large amount of work modeling the displacement of one fluid by another in porous media but only limited papers related to CO<sub>2</sub>-brine flow. Aside from our work existent studies of CO<sub>2</sub> injection into brine only consider single well injection cases and the main efforts have been dedicated on CO<sub>2</sub> migration (to address plume extent and the fate of leakage) rather than pressure build up in the entire reservoir.

The spectrum of studies related to modeling of pressure evolution during CO<sub>2</sub> injection can be represented by two limits: i) oversimplified analytical models, by trying to use existing pressure profile solutions for single-phase flow and adjusting them to two-phase pressure build up, with differing approximations for different regions around the injector, for example [6, 7]; and ii) a general formulation which even in the one-dimensional case and using common assumptions requires numerical contributions in evaluating pressure profile.

There are only few studies on analytical modeling of multiple well scenarios for CO<sub>2</sub> injection in a geological formation, for example [8, 9]. In these studies single-phase steady state flow and the superposition technique were used to account for multi-well injection and the effects of two-phase flow were not considered.

In our previous study [4], we developed an approach which considers two-phase (CO<sub>2</sub> and brine) flow and extended it to multi well injection scenarios. Since we are using this approach in the current study a short summary of this approach is presented below. First, solution for a single injector is presented and then it is extended to the multi-well injection case.

## 2.2 Solutions to the Diffusivity Equation for a single injection well

First, a single well solution is found for one dimensional radial case. The assumptions include a horizontal, homogeneous and isothermal aquifer with constant fluid properties. Capillarity and gravity are neglected, vertical (from top to bottom) line type injection is assumed, and both fluids are considered to be slightly compressible. These assumptions allow us to obtain an analytical injection solution by solving the diffusivity equation for pressure distribution in all three regions established during CO<sub>2</sub> injection (CO<sub>2</sub> region (dr), two-phase Buckley-Leveret (BL) region, and the brine region [10], Figure 1 below.

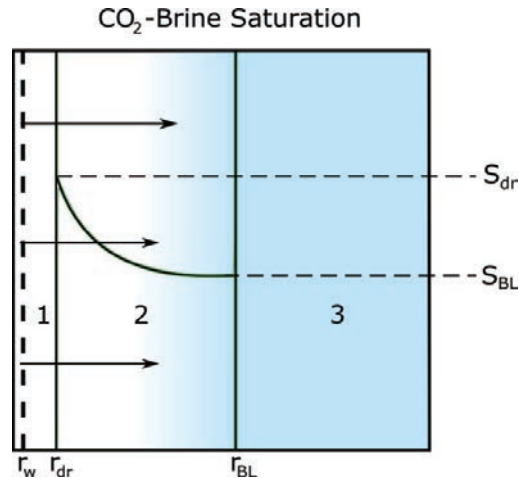


Figure 1: Schematic of single well injection CO<sub>2</sub> injection: 1 – CO<sub>2</sub> region, 2 – Two-phase region, 3 – Brine region

CO<sub>2</sub> Region:  $\xi \leq \xi_{dr}$

$$P_1 = -\frac{1}{2} E_i(-\xi) + \frac{1}{2} E_i(-\xi_{dr}) - \frac{1}{2F_{\lambda_g}} E_i\left(\frac{-\xi_{dr}}{F_{\lambda_g} \eta_{D2}}\right) + \frac{1}{F_{\lambda_g}} E_i\left(\frac{-\xi_{BL}}{F_{\lambda_g} \eta_{D2}}\right) - \frac{\bar{\lambda}_g}{2\lambda_w} E_i\left(\frac{-\xi_{BL}}{\eta_{D3}}\right) \quad (1)$$

Two-phase Region:  $\xi_{dr} < \xi \leq \xi_{BL}$

$$P_2 = -\frac{1}{2F_{\lambda_g}} E_i\left(\frac{-\xi}{F_{\lambda_g} \eta_{D2}}\right) + \frac{1}{F_{\lambda_g}} E_i\left(\frac{-\xi_{BL}}{F_{\lambda_g} \eta_{D2}}\right) - \frac{\bar{\lambda}_g}{2\lambda_w} E_i\left(\frac{-\xi_{BL}}{\eta_{D3}}\right) \quad (2)$$

Brine Region:  $\xi > \xi_{BL}$

$$P_3 = -\frac{\bar{\lambda}_g}{2\lambda_w} E_i\left(\frac{-\xi}{\eta_{D3}}\right) \quad (3)$$

The parameters and variables used in the above system and in following text are defined in Nomenclature.

$$P_D = (P - P_i) \frac{2\pi h k \overline{k}_{rg}}{q \mu_g B_g}, \quad t_D = t \frac{\overline{k k}_{rg}}{\mu_g r_w^2 \phi c_{tg}}, \quad r_D = \frac{r}{r_w}, \quad \varepsilon = \frac{q \mu_g B_g c_{tg}}{4\pi h k \overline{k}_{rg}}$$

The system of Equations (1) – (3) consists of three separate solutions for the diffusivity equation, one for each region (Fig.1), but it does not define the boundaries of the two-phase region  $BL$  and  $dr$ .

The main benefit of the above formulation is that the solutions in all three regions have the dimensionless similarity form  $\xi = r_D^2/4t_D$  and so boundaries of regions are constants and can be found separately. The values of the similarity form are calculated using specific fluid and rock properties within a particular reservoir.

### 2.3 Boundaries of the Two Phase Region for a single well

The understanding of immiscible flow in a two-phase flow is usually addressed by the Buckley-Leverett (BL) fractional flow theory [11]. This theory allows estimation of the saturation profile and requires knowledge of the fractional flow function [12]:

$$f_g = \frac{1}{1 + \left(\frac{k_{rg}}{k_{rw}}\right) \left(\frac{\mu_w}{\mu_g}\right)} \quad (4)$$

One can see that the equation depends on reservoir rock and fluid properties which are particular for each case under consideration. A variety of methods exist to evaluate flow region boundaries and they are discussed in the results section.

### 2.4 Multiple Injection Well Scenarios

As was previously mentioned, there are various analytical models proposed for single wells to determine the pressure profile for CO<sub>2</sub> injection in saline formations. However, in order to inject a large amount of CO<sub>2</sub>, more than one well is required. The principal of superposition is employed to account multi-well injection scenarios:

$$p(r, t) = \sum_{n=1}^n p_n(r_n - r, t) \quad (5)$$

Equation (5) states that the pressure at any point ( $r$ ) and at any time ( $t$ ) in the reservoir can be represented by the superposition of solutions  $p_n$  for each individual injector, calculated by the single well model.

## 3. Results – Optimization of injection well capacity

In this section the above modeling is used to optimize the injection capacity of saline aquifers. First the boundaries of the two phase region are found using the method outlined in section 2.3 above. Two cases are considered: i) hypothetical aquifer (mentioned in our paper as Berkeley) based on the data set of inter-comparison study [5] initially designed by the Lawrence Berkeley National Laboratory and ii) the real aquifer (Nisku), which is located in Alberta, Canada.

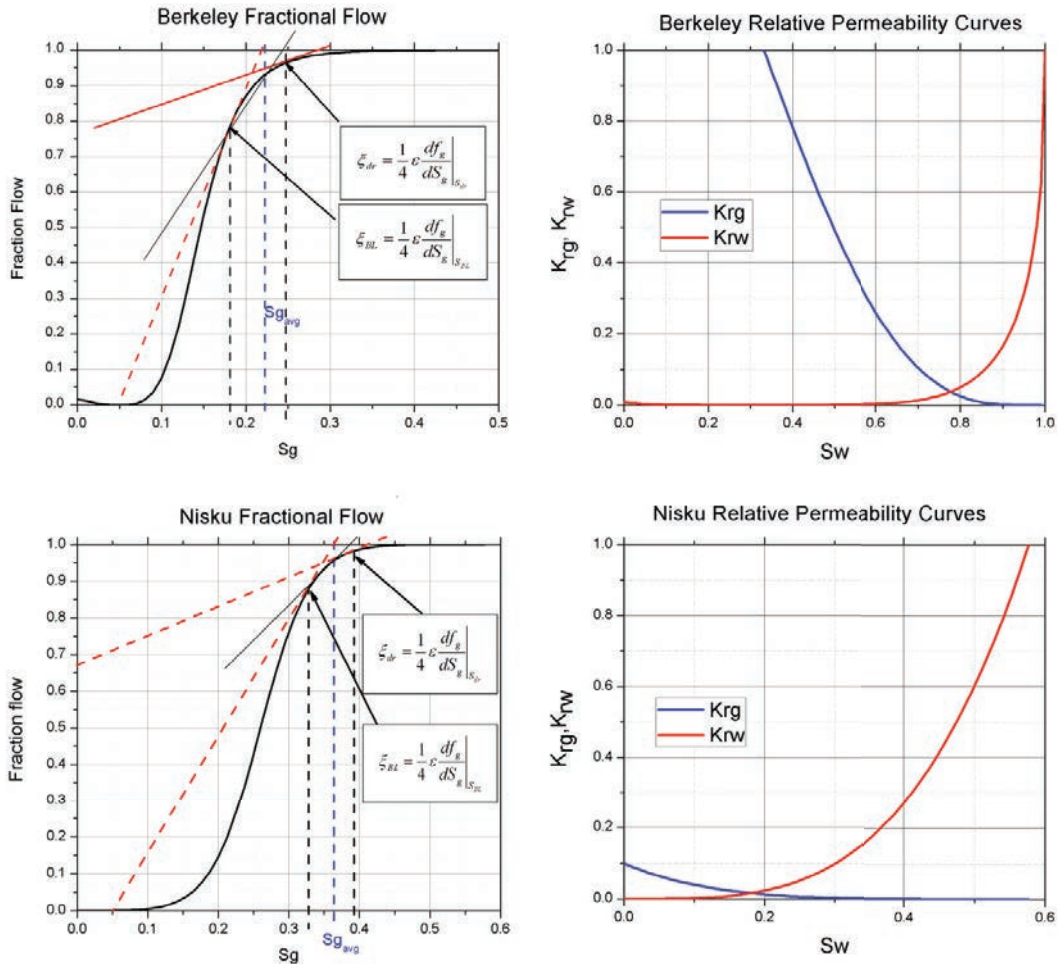


Figure 2: Fractional flow and corresponding relative permeability curves. For the Berkeley relative permeability curves Corey type and van Genuchten functions were used to define the curves while the Nisku formation relative permeability were experimentally determined.

For the Berkeley formation the fractional flow curve was generated from relative permeability curves defined by the Corey type function [13] (gas relative permeability) and the van Genuchten function [14] (brine relative permeability) and the data set of study [5] while for the Nisku formation experimentally determined relative permeability curves were used.

The fractional flow functions, based on equation (4), are plotted (solid black curves) using the corresponding relative permeability curves (Fig. 2). From the fractional flow graphs, locations of two-phase region boundaries ( $\zeta_{dr}$  and  $\zeta_{BL}$ ) as well as saturations at the boundaries ( $S_{dr}$  and  $S_{BL}$ ) for both aquifers can be evaluated. Tangents (red lines) to the fractional curves through the point at which  $f_g=0$ , this corresponds to  $S_{gr}$  the residual saturation of  $CO_2$ . The average saturation of  $CO_2$  ( $S_{av}$ ) is determined by the intersection of this tangent line and  $f_g=1$  according to study [15]. Extending the lines formed by joining the points  $f_g(S_{BL})$  and  $f_g(S_{av})$  and finding its intersections with  $f_g=1$  line gives corresponding  $S_{dr}$ . The tangents to the fractional flow curves at  $S_{dr}$  and  $S_{BL}$  give  $\zeta_{dr}$  and  $\zeta_{BL}$  for both formations as shown in Fig. 2.

There are several other methods that can be used to define the location of tangent lines to the fractional curve, corresponding to the boundaries of the two-phase region such as those proposed in [16, 17]. We previously compared the methods and found that Welge's method [12] provides the closest result to numerical simulations [4]. As any analytical approach requires validation against numerical simulations, we determined the regions by first approximating them using Welge's method and then fitting the edges of the boundaries to numerically determined fracture pressure data. We previously performed sensitivity testing comparing our semi-analytic model to simulations [2] with good agreement [4]. Once calibrated these boundaries are kept constant and used for multiple well modeling without any further numerical simulations and adjustments.

After the boundaries were identified, the pressure distribution was then generated from the solutions to the diffusivity equations above (1) – (3) combined with the superposition principle (5). The reservoir properties that were used in each case are listed below in Table 1.

Table 1: Properties used in semi-analytically modeling of CO<sub>2</sub> injection wells.

Properties	Berkeley	Nisku
Initial Pressure ( $P_i$ )	$1.2 \times 10^7$ Pa	$1.6 \times 10^7$ Pa
Fracture Pressure ( $P_f$ )	$3.0 \times 10^7$ Pa	$3.0 \times 10^7$ Pa
Flow Rate ( $q$ )	81.02	17.04
Reservoir Temperature ( $T$ )	45 °C	54 °C
Porosity ( $\phi$ )	0.12	0.064
Permeability ( $k$ )	100 mD	43 mD
Thickness ( $h$ )	100 m	102 m
Rock Compressibility ( $c_r$ )	$1.45 \times 10^{-7}$ 1/Pa	$1.45 \times 10^{-7}$ 1/Pa
Brine Compressibility ( $c_w$ )	$1 \times 10^{-9}$ 1/Pa	$1 \times 10^{-9}$ 1/Pa
CO <sub>2</sub> gas formation volume factor ( $B_g$ )	0.022	0.022
Brine residual saturation ( $S_{wr}$ )	0.332	Not used
CO <sub>2</sub> residual saturation ( $S_{gr}$ )	0.05	Not used
Brine viscosity ( $\mu_w$ )	0.84 cP	0.74 cP
CO <sub>2</sub> viscosity ( $\mu_g$ )	0.062 cP	0.07 cP
Relative gas permeability at $S_g=0$ ( $\overline{k_{rg}}$ )	0.80	0.80

Below are results of modeling of efficiency of CO<sub>2</sub> injection design which depends on number of wells, distance between the wells and their injection rates. The efficiency can be defined as injection capacity, maximum amount which can be injected within specific period of time (which in our study 50 years of injection). The maximum amount is controlled by fracture pressure of reservoir cap-rock. In the study the maximum pressure is set to 0.9 of fracture pressure as required by regulations to keep integrity of a formation.

First, for both reservoirs the capacities of injection for different number (1-25) of equally spaced injectors which inject at the same flow rate have been investigated. Then optimization of flow rates for each injector has been made and substantial increase was observed for both reservoirs.

The pressure distributions at maximum constant flow rates for both aquifers are shown on Figures 3 and 4.

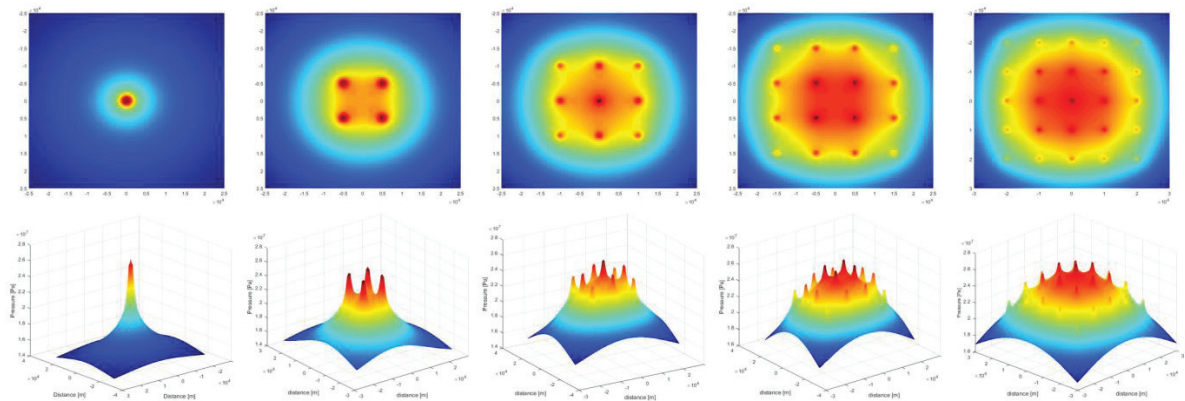


Figure 3: Berkeley pressure distributions for each of the well configurations with the same injection rate at each wellbore over a  $60 \text{ km} \times 60 \text{ km}$  reservoir area with a maximum peak pressure of 27 MPa.

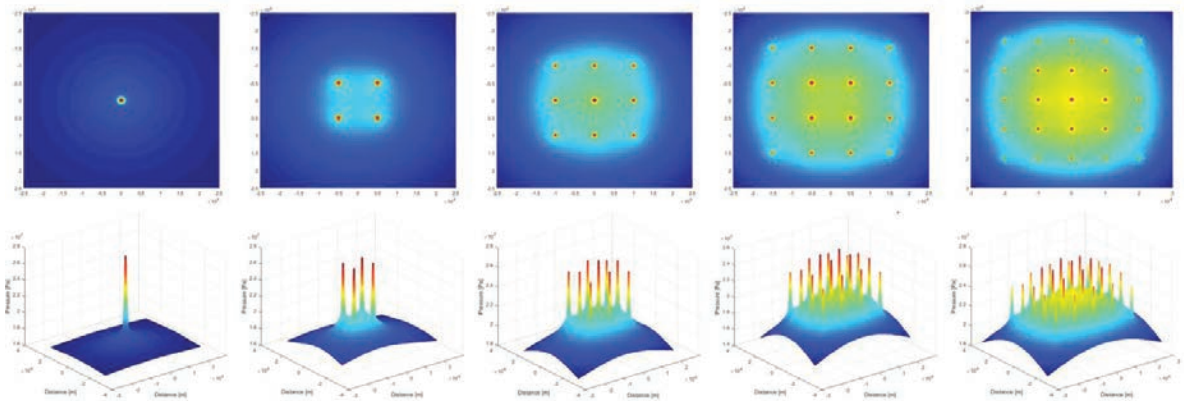


Figure 4: Nisku pressure distributions for each of the well configurations with the same injection rate at each wellbore over a  $60 \text{ km} \times 60 \text{ km}$  reservoir area with a maximum peak pressure of 27 MPa.

As can be seen from the Nisku pressure distributions a reduction in porosity, formation permeability and the resulting changes in saturation profiles result in much sharper increases in pressure moving toward any wellbore. This has important consequences on the pressure distribution within the injection well reducing injection capacity. In our model we assume an infinite acting boundary which is not the case for the real Nisku formation. Although Nisku formation is very big with about 450 km east west and 600 km south north extend, it is irregularly shaped, and the area where the reservoir data were collected is narrow (about 30 km south north extend). The boundary effects can be modeled by placing imaginary wells around injection area of the formation to satisfy no flow conditions at the boundary of aquifer. From the Nisku pressure distributions shown here it can be seen that the effects of well interference are not as pronounced – likely due to the reduction in porosity and permeability of the formation. We can then extend this to assume that the boundaries of the formation will have a less significant effect on the pressure within the well for the Nisku formation than the Berkeley formation which has a much higher permeability and porosity. Unfortunately, significantly less benefit in total injection capacity is observed due to lower permeability when optimizing well injection rates.



3.2 Optimization of injection capacity

Optimal injection rates at each well depend not only on the physical properties of the aquifer such as porosity, size and permeability of the formation, but also on the well configuration and their flow rates. Figure 5 shows the degeneracy in injection rates at each of the wellbores for each well configuration. In the 1 and 4 well cases there is no degeneracy and therefore the optimal injection rate is the same as in the case above.

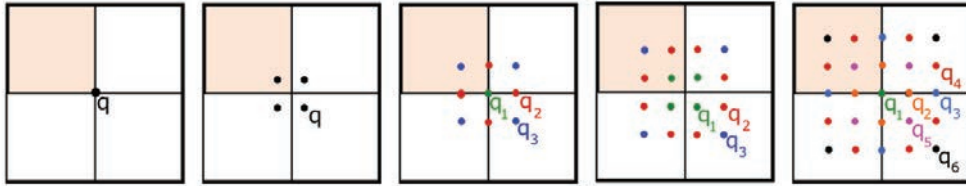


Figure 5: Degeneracy in the injection rates for up to 25 wells

In the 9, 16 and 25 well cases injection rates can be optimized. In the cases 9 and 16 wells three rates to be varied (due to symmetry) and for the case of 25 wells, six flow rates are to be defined. The resulting pressure fields are presented on Figures 6 and 7.

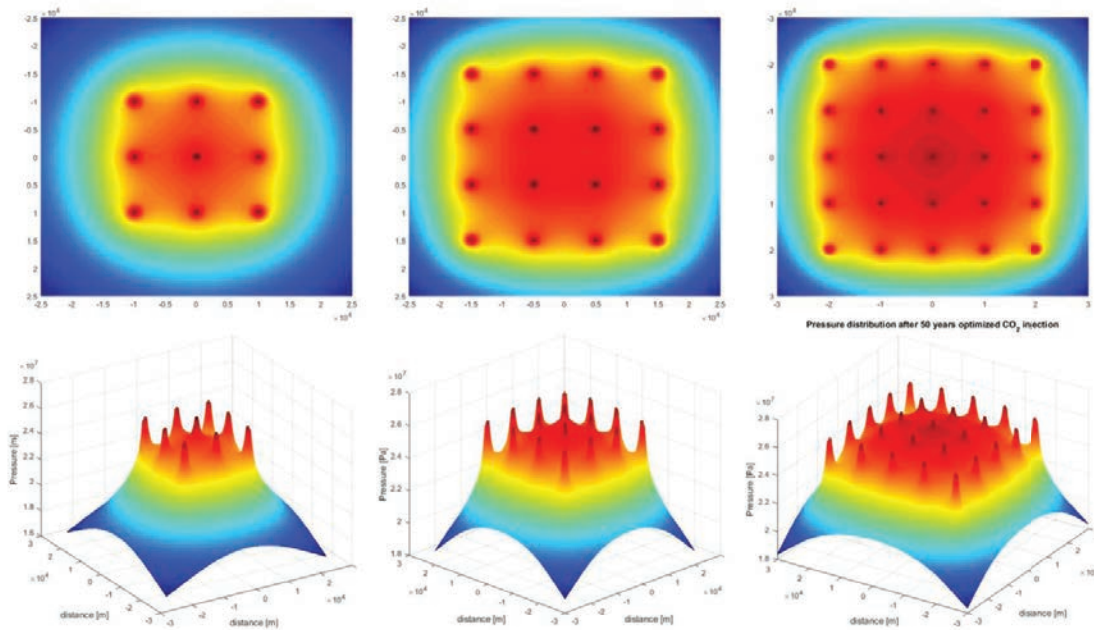


Figure 6: Pressure distribution after optimization of injection rates to maximum allowable pressure (27 MPa) for the Berkeley formation

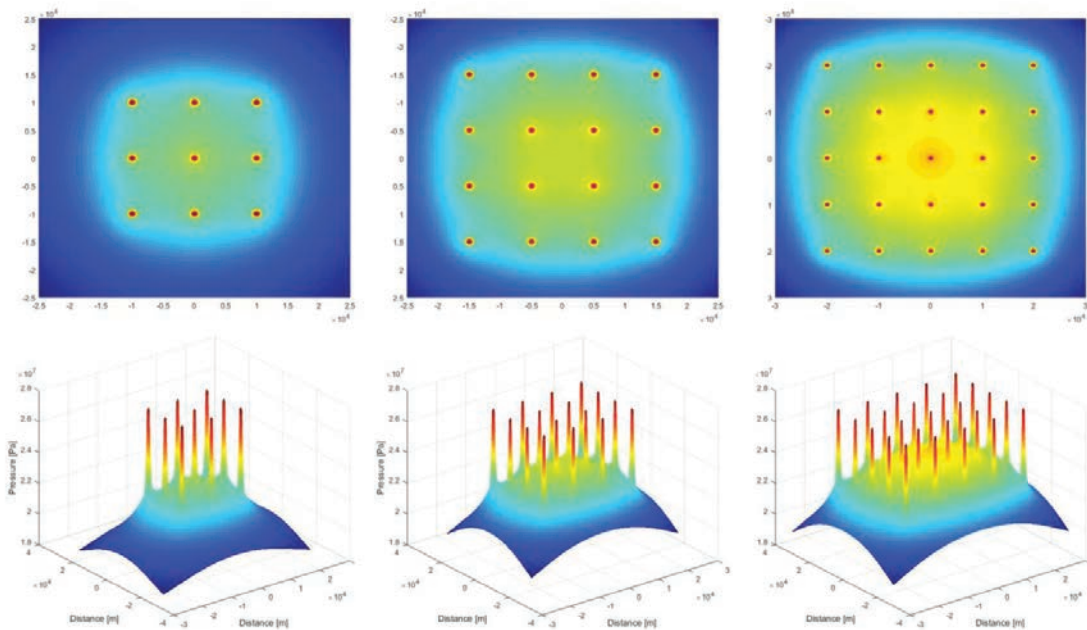


Figure 7: Pressure distribution after optimization of injection rates to maximum allowable pressure (27 MPa) for the Nisku formation

Increased injection capacity by optimization of the wellbore injection rate is shown in Figures 8 below. Unsurprisingly reduction in basic well injection capacity due to the physical properties of the injection formation reduces the advantage of optimization of the injection rates at each wellbore.

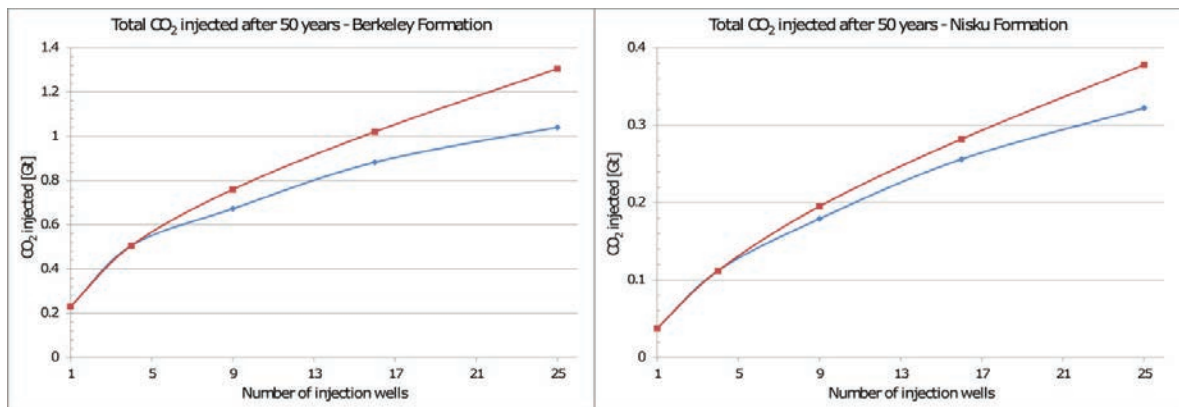


Figure 8: Injection capacity of the Berkeley (left) and Nisku (right) formations before (blue) and after (red) optimization of injection rate at each wellbore.

#### 4. Summary and conclusions

To make geological disposal a viable option for the reduction of CO<sub>2</sub> emissions, large volumes of sequestration have to be considered. It creates large scale pressure increases during injection period and could impact formation

integrity. Pressure management becomes much more challenging since it requires multiple injector designs. The number of variables substantially increases thus increasing the number of design strategies. The development of fast tools to be able to screen design strategies becomes very essential.

In this study we show how such approach can be used to optimize injection rates during multiple well injection into deep aquifers. Modeling is based on solutions of the diffusivity equation for slightly compressible fluids for three regions developed during single well CO<sub>2</sub> injection. The boundaries of the three regions are found separately by using Buckley-Leverett theory and by fitting values of BHP that were determined numerically and kept the same for multiple well cases. Then solutions for the single well case have been extended to multiple well injection by using the principle of superposition.

Described approach can be used as a screening tool for fast aquifer capacity evaluation when large volumes are considered and multiple well designs are required. It can be used for the optimization of well number and their placement as well as their flow rates. It significantly reduces the time required in comparison to traditional reservoir simulations.

### Acknowledgements

Financial support for this work provided by CMC (Carbon Management Canada Research Institutes)

### References

- [1] IPCC (Intergovernmental Panel on Climate Change). Special Report on Carbon Capture and Storage. Cambridge University Press; 2005.
- [2] Ghaderi S, Keith D, Leonenko Y. Feasibility of Injecting Large Volumes of CO<sub>2</sub> into Aquifers. *Energy Procedia* 2009;1(1): 3113-3120.
- [3] Ghaderi SM, Leonenko Y. Reservoir modeling for Wabamun lake sequestration project. *Energy Science & Engineering* 2009;3(2): 98-114.
- [4] Joshi A, Gangadharan S, Leonenko Y. Modeling of pressure evolution during multiple well injection of CO<sub>2</sub> in saline aquifers. *Journal of Natural Gas Science and Engineering* 2016; doi: 10.1016/j.jngse.2016.06.005.
- [5] Pruess K, Garcia J, Kovscek T, Oldenburg C, Rutqvist J, Steefel C, Xu T. Code inter-comparison builds confidence in numerical simulation models for geologic disposal of CO<sub>2</sub>. *Energy* 2004;29(9):1431-1444.
- [6] Ehlig-Economides C, Economides M. Sequestering carbon dioxide in a closed underground volume. *J. Petrol. Sci. Eng.* 2010;70(1):123-130.
- [7] Mijic A, LaForce TC, Muggeridge AH. CO<sub>2</sub> injectivity in saline aquifers: The impact of non-Darcy flow. *Water Resources Research*. 2014;50:4163-4185.
- [8] Zakrisson J, Edman I, Cinar Y. Multiwell injectivity for CO<sub>2</sub> storage. SPE Asia Pacific Oil and Gas Conference and Exhibition, 20-22 October, Perth, Australia; 2008.
- [9] Pooladi-Darvish M, Moghdam S, Xu D. Multiwell injectivity for storage of CO<sub>2</sub> in aquifers. *Energy Procedia* 2011;4:4252-4259.
- [10] Azizi E, Cinar Y. Approximate analytical solutions for CO<sub>2</sub> injectivity into saline formations. *SPE Reserv. Eval. Eng.* 2013;16(2): 123-133.
- [11] Buckley S, Leverett M. Mechanism of fluid displacement in sands. *Trans. AIME* 1941;146(1):107-116.
- [12] Dake LP. *Fundamentals of Reservoir Engineering*. Elsevier Science; 1978.
- [13] Corey AT. The Interrelation Between Gas and Oil Relative Permeabilities, *Producers Monthly*; November 1954:38-41.
- [14] Van Genuchten MT. A Closed-Form Equation for Predicting the Hydraulic Conductivity of Unsaturated Soils, *Soil Sci. Soc. Am. J.* 1980;44:892 – 898.
- [15] Welge H. A simplified method for computing oil recovery by gas or water drive. *J. Petrol. Technol.* 1952;4(4):91-98.
- [16] Noh M, Lake L, Bryant S, Araque-Martinez A. Implications of coupling fractional flow and geochemistry for CO<sub>2</sub> injection in aquifers. *SPE Reserv. Eval. Eng.* 2007;10(4):406-414.
- [17] Woods E, Comer A. Saturation distribution and injection pressure for a radial gas storage reservoir. *J. Petrol. Technol.* 1962;14(12):1-389.